

Aqueous processing of natural graphite particulates for lithium-ion battery anodes and their electrochemical performance

Jin-Hyon Lee^a, Sangkyu Lee^a, Ungyu Paik^{a,*}, Young-Min Choi^b

^a Department of Ceramic Engineering, Hanyang University, Seoul 133-791, Republic of Korea

^b Materials LAB, Samsung Advanced Institute of Technology, P.O. Box 111, Suwon 440-600, Republic of Korea

Received 8 October 2004; accepted 18 January 2005

Available online 9 March 2005

Abstract

Aqueous-based natural graphite particulates for fabrication of lithium-ion battery anodes are investigated with emphasis on chemical control of suspension component interactions among graphite particulates, sodium carboxymethyl cellulose (CMC), and emulsified styrene butadiene rubber (SBR). The chemical stability and dispersion properties of the natural graphite particles are characterized using electroacoustic, flow behaviour and green microstructural observations, as well as by measurement of pore size. Correlation is made between the dispersion characteristics and the electrochemical performance of the particles. The dispersion stability of the graphite suspension is improved by charge development when both SBR and CMC are incorporated into the graphite suspension, compared with an unstable graphite suspension prepared with CMC alone. A method to improve the dispersion and homogeneity of the suspension component based on the use of SBR and CMC is proposed. Electrochemical experiments using a Li-organic electrolyte-as-cast natural graphite half-cell and 750-mAh lithium-ion cells show an initial discharge capacity above 340 mAh g^{-1} , improved charge-discharge efficiency, and excellent rate capability.

© 2005 Elsevier B.V. All rights reserved.

Keywords: Lithium-ion battery; Aqueous processing; Natural graphite particles; Carboxymethyl cellulose; Styrene butadiene rubber

1. Introduction

Tape casting is widely used in the fabrication of lithium-ion batteries [1]. Production of electrode tapes with a high packing density and a homogeneous green microstructure is dependent on the stability and chemistry of the particulate suspension. To obtain a suspension suitable for tape casting, organic solvents have traditionally been used as the suspending medium. Since, organic solvents are typically flammable and environmentally unfriendly, careful handling is required. This gives rise to both cost and safety concerns [2]. Recently, an attempt has been made to switch from a non-aqueous to an aqueous based system.

The transition from a non-aqueous to an aqueous tape-casting process may involve unexpected difficulties in preserving the electrical properties for battery applications.

These problems mainly originate from the distinct physicochemical properties between organic additives at the solid-liquid interface. In addition, slurry formulations that are compliant with the suspended medium, including the binder and other functional additives, have to be newly determined. Therefore, this study focuses, on a graphite anode cast on a copper foil and investigates both colloidal stability in an aqueous medium and the electrochemical performance.

Among the various carbonaceous materials, such as natural and artificial graphite [3,4], pitches, cokes and meso-carbon microspheres, that can be considered for use as anode materials, natural graphite is very promising due to its advantages of high capacity at a low and flat potential and low cost [5]. Casting of an aqueous graphite slurry does, however, give rise to the need to find a suitable binder that is compatible with an aqueous-based system. In addition to being chemically and electrochemically stable in a given electrode-electrolyte system, the binder has to accommodate the large dimensional changes that occur during operation of the electrodes [6].

* Corresponding author. Tel.: +82 2 2290 0502; fax: +82 2 2281 0502.
E-mail address: upaik@hanyang.ac.kr (U. Paik).

Previous research has reported that polyvinylidene difluoride (PVDF) has been used as a binder for graphite anodes because of its good electrochemical stability and its ability to adhere to electrode material and copper current-collectors [1,7]. In the present investigation, a water-soluble cellulose derivative, sodium carboxymethyl cellulose (CMC), is used as the binder. CMC is a linear polymeric derivative of cellulose and consist of β -linked glucopyranose residues with varying levels of carboxymethyl ($-\text{CH}_2\text{COO}^-$) substitution [8]. The presence of the carboxymethyl groups is responsible for the aqueous solubility of CMC relative to insoluble cellulose. CMC is a weak polyacid that dissociates to form carboxylate anion functional groups. The degree of substitution (DS) is most commonly in the range of 0.6–0.95 derivatives per monomer unit, but derivatization is not evenly distributed along the chain, and regions of high and low substitution are known to exist. The other predominant functional group on CMC is the hydroxyl, which is replaced by the carboxymethyl group during derivatization [9–11]. Cellulose derivatives have been applied in the fabrication of separators in various types of batteries, such as lead–acid [12,13]. CMC and emulsified styrene butadiene rubber (SBR) have been widely used as organic additives in the fabrication of positive and negative electrodes for aqueous or non-aqueous nickel–metal-hydride, nickel–cadmium, and lithium-ion batteries [14–16].

The present work examines the effect of CMC and SBR on the dispersion and tape-casting properties of natural graphite particulate in an aqueous medium by investigating the electrokinetic, rheological and swelling behaviour, as well as by conducting scanning electron microscope observations and mercury porosimetry measurements. Following these studies, the electrochemical performance of a 750-mAh lithium-ion battery, which employs a natural graphite anode fabricated from the aqueous slurry formulation and a LiCoO_2 cathode, is evaluated.

2. Experimental

Natural graphite powder was obtained from commercial sources (90%, SL-20, Superior Graphite Company, Japan) and had a mean particle diameter of 5–20 μm . The density as stated by the manufacturer was 2.245 g cm^{-3} . CMC (Daicel Co. Ltd., Japan) with an average molecular mass of 330,000, and a degree of substitution of $\text{DS} = 1.28$, and SBR (SB131, Zeon Corporation, Japan) with a solids loading of 40 wt.% were used as the organic additives.

Suspensions containing a 5% solids weight fraction were ultrasonically dispersed for 3 min using a submersible titanium horn, and then allowed to equilibrate for 12 h before electrokinetic measurements were performed. The electrokinetic behaviour of the graphite suspensions containing CMC, both with and without SBR, was characterized as a function of the concentration of the organic additives by means of an

electroacoustic technique (Model ESA-9800, Matec Applied Sciences, Hopkinton, MA).

Suspensions containing a solids weight fraction of 35% were also ultrasonically dispersed for 3 min using a submersible titanium horn, and then allowed to equilibrate for 12 h before carrying out rheological measurements. The rheological behaviour of graphite suspensions containing CMC, with and without SBR, were measured at a temperature of $20 \pm 0.1^\circ\text{C}$ using a controlled stress rheometer (MCR 300, Paar Physica, Stuttgart, Germany) to assess the stability of the suspensions. A concentric cylinder (CC 27) geometry bob (bob radius = 13 mm, cup radius = 14 mm) was utilized and measured stresses in the range of 0–1000 Pa. Two types of viscosities, viz., the apparent and the relative viscosity, were measured and calculated. The apparent viscosity was determined as a function of CMC concentration. To calculate the relative viscosity, the viscosity of the suspending liquid medium was measured after the suspensions had been centrifuged. Each measurement of the polymer solutions was performed using a fresh aliquot of suspension. The sedimentation time was calculated according to Stokes' equation, when the graphite particles had settled to a depth of 1 cm. The gel samples were dried to a constant weight and immersed in distilled water for 12 h at room temperature and then the weights of the swollen gel samples were determined. The pH of the solution was monitored.

The suspensions were cast on to copper substrates using a laboratory-scale doctor blade machine. A gap height of $\sim 230 \mu\text{m}$ was used, and the casting speed was held constant at 5 m per minute. The tapes were dried in stagnant air for a period of 24 h, cut into rectangular samples (2.5 cm^2), and removed from the carrier film. The fracture regions of representative as-dried films, both with and without SBR, were examined using a scanning electron microscope (SEM, JSM 5900LV, Jeol, Tokyo, Japan). A small portion from each dried film was mechanically removed and transferred into a sample holder. It was then fast-frozen with liquid nitrogen and fractured to yield an observable sample. The samples were gold-coated and examined in the SEM, which operated at an accelerating voltage of 20 kV. In addition, the pore size and distribution of the as-dried sheets were measured with a mercury porosimeter (Autoscan-25, 60, Quantachrome Corp., Suppset, NY, USA).

Charge–discharge experiments were conducted at room temperature using a three-electrode electrochemical cell. Two types of electrode sample made from natural graphite and artificial graphite served as the working electrodes. One electrode was an SBR-bonded graphite electrode composed of a natural graphite powder, and the other electrode was a PVDF-bonded graphite electrode composed of artificial graphite powder. Pure lithium metal foil (Cyprus-Foote Mineral Co., Kings Mountain, NC, USA) was employed as the reference and counter electrodes. The electrolyte was 1.1 M LiPF_6 in a 3:6:1 vol mixture of ethylene carbonate (EC), ethyl–methyl carbonate (EMC), and di-methyl carbonate (DMC). Lithium charge–discharge curves were measured using a computer-

ized multi-channel battery charger (HRC 6064A, Toyo System Co., Ltd., Fukushima, Japan). The galvanostatic charge and discharge currents corresponded to a unit change of x in Li_xC_6 in 10 h.

Finally, the rate capability of a 750-mAh lithium-ion cell employing a natural graphite anode and an LiCoO_2 cathode was evaluated from discharge characteristics at various current densities.

3. Results and discussion

The pH-dependent electrokinetic behaviour of graphite suspensions in an aqueous medium prepared with CMC is presented in Fig. 1. SBR has not been added to these suspensions. To obtain an understanding of the effect of CMC on the stability of graphite particles in an aqueous medium, the surface potentials of native graphite suspensions (i.e., in the absence of organic additives) as well as that of CMC-containing graphite suspensions has been evaluated. It is not possible, however, to obtain reliable electrokinetic sonic amplitude (ESA) measurements on aqueous suspensions of native graphite due to the small ESA signals. Even in the presence of moderate stirring, graphite particles in an aqueous medium settle out within a few minutes, as graphite particles have a hydrophobic nature. Furthermore, graphite has a relatively high Hamaker constant of 47×10^{-20} J [17,18], which is directly proportional to the van der Waals attractive interaction energy. Therefore, aqueous suspensions of native graphite (i.e., in the absence of organic additives) are completely unstable, and rarely develop a surface potential by adsorbing potential-determining ions, H_3O^+ or OH^- [18]. This incompatibility of native graphite with water should be resolved in order to employ graphite in place of lithium as an anode material in an aqueous process for cell manufacture. Therefore, CMC has been used in the present investigation in order to improve the stability of native graphite particles in an aqueous medium.

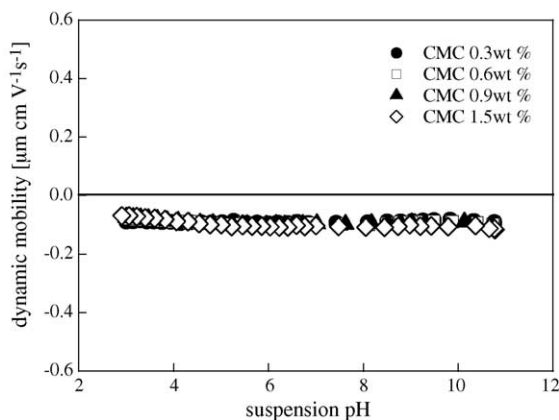
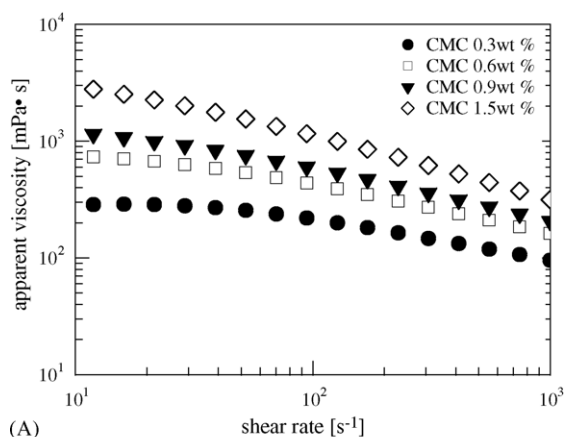


Fig. 1. Electrokinetic behaviour of graphite suspensions with CMC prepared with a mass fraction of 5 wt.% solids content. The CMC content of the suspensions is varied for mass fractions 0.3–1.5 %, based on solids content.

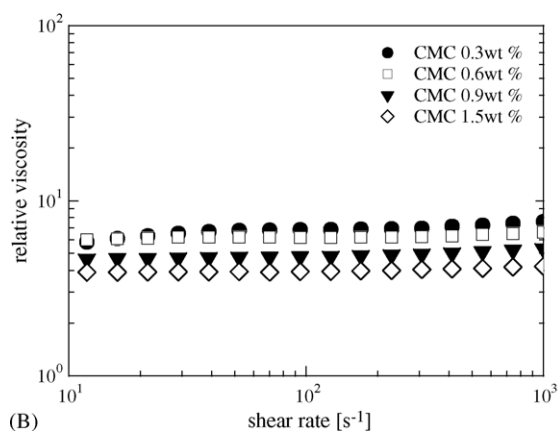
Cellulose is a non-toxic and biodegradable polymer, and has been recently used as an additive in electrodes for advanced batteries and in papermaking [19,20]. In particular, CMC is attracting interest as a potential binding material for graphitic anodes in lithium-ion batteries [8,9,14–16], since CMCs are used for film formation capacity, which is related to the improvement of strength and flexibility of green sheet. In addition, the adsorption behaviour can be easily adjusted by changing the electrostatic environment, such as the electrolyte concentration or the hydrogen ion concentration [11]. Electrokinetic curves (see Fig. 1) indicate that the graphite particles in the presence of CMC exhibit a negative potential across the normal pH range. This is attributed to the presence of the carboxylate functional groups within the adsorbed layer of CMC, which contribute to an effective surface layer charge on graphite. It is well known that the carboxylic acid unit of CMC can be dissociated into a carboxyl group and a hydrogen ion in water as a function of pH [21]. The ionized CMC present on the solids contributes to the development of a surface potential within the suspension. In addition, the adsorption of CMC on to graphite can be driven through a hydrophobic interaction, because the graphite particles have a hydrophobic surface property [18,22].

The electrophoretic mobility of graphite was found to be independent of the CMC concentration, as shown in Fig. 1. A small divergence in the mobility value is within the experimental error for this measurement, estimated at $\pm 0.05 \mu\text{m cm V}^{-1} \text{s}^{-1}$ [22,23]. The independence with respect to CMC concentration can be explained in terms of the electrokinetic shear-plane. Only the near-surface fraction of carboxylate sites will contribute to the shear plane potential that is responsible for the ESA response. By contrast, it was not possible to measure electrokinetic curves for graphite suspensions prepared with SBR in the absence of CMC. SBR exists as a soluble latex particle with a negative surface charge due to fatty acid [24], and is therefore not likely to interact with the hydrophobic graphite particles. Thus, suspensions prepared with SBR are unstable and only the graphite phases settled out during the measurements.

Logarithmic plots of the apparent viscosity (A) and log-plots of the relative viscosity (B) are shown in Fig. 2 for graphite suspensions prepared with CMC as a function of the CMC concentration at $\text{pH } 7.5 \pm 0.3$. All the suspensions were prepared at a 35 wt.% fraction of solids, along with CMC in an aqueous medium. From Fig. 2A, the suspensions exhibit a linear dependence of the viscosity on the shear rate, i.e., a ‘shear thinning’ behaviour at all CMC concentration. The shear thinning of the concentrated suspensions appears because of the break-down of agglomerates by the applied shear force, which eventually reduces the viscosity [25]. And the apparent viscosity of the suspension increases with increasing polymer concentration. It is reported that CMC by virtue of its network structure plays the role of a thickener (namely, flocculating agent) as well as a surface modifier [6,26]. The substitution of a viscous binder solution for a simple liquid thickens the system, and thereby, increases the apparent



(A)

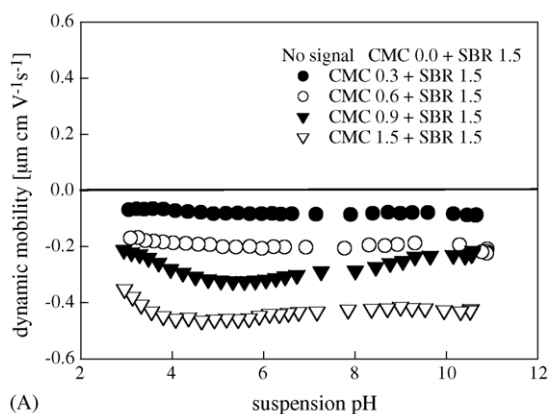


(B)

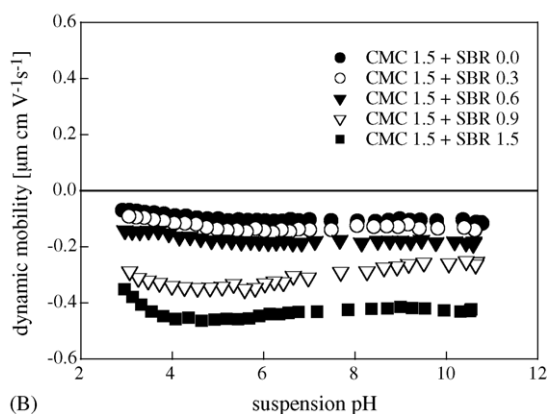
Fig. 2. Logarithm plot of viscosity versus shear rate for graphite suspension with mass fraction of 35% solids content prepared with CMC alone: (A) apparent viscosity and (B) relative viscosity.

viscosity. This is because celluloses in water form highly adhesive structures in suspension. On the other hand, log-plots of relative viscosities (Fig. 2B), which differentiate the particle–particle interactions from the collective contribution of all the components in solution, display Newtonian-like fluid behaviour regardless of the additive concentration. As more CMC is added to the suspensions, the relative viscosity slightly decreases, which results from a decrease in the particle–particle interactions.

The pH-dependent electrokinetic curves for graphite suspensions in the presence of CMC with SBR are presented in Fig. 3 as a function of additive concentration. It is remarkable that the dynamic mobility of these suspensions increases when CMC and SBR added together in increasing amounts to graphite suspensions. This observation is quite different from the electrokinetic behaviour of suspensions prepared with either CMC or SBR in a separate formulation. These remarkable phenomena can be explained in terms of the re-orientation of carboxymethyl units and the electrokinetic shear-plane. The carboxymethyl units in the CMC and the carboxylic groups in the SBR can dissociate in water and thereby form charges at the tails of dissociated units. The repulsive force between the COO^- side-group in CMC and



(A)



(B)

Fig. 3. Electrokinetic behaviour of graphite suspension prepared with mass fraction of 5 wt.% solids content with various additives: (A) CMC and (B) CMC (at fixed mass fraction of 1.5%) and SBR at mass fraction based on solids content.

the surface COO^- on SBR latex forces them away from each other so as to increase their configurational entropy. The repulsive force between like-charged units was reported for a polymerized crystalline colloidal array (PCCA) that has a crown ether-cation [27]. The freedom of the COO^- side-group in CMC is restricted, however, because CMC is adsorbed on the graphite surface via hydrophobic–hydrophobic interaction between the backbone of the CMC and the hydrophobic graphite surface. Therefore, partial rotation of the $\text{CH}_2\text{OCH}_2\text{COOH}$ side-group in CMC around the C–C bond linking the group to the backbone of CMC is expected so as to increase the configurational entropy. Eventually, partial rotation of the carboxymethyl units in CMC will contribute to increasing the near-surface fraction of carboxylate sites in CMC, which is responsible for the increase in surface potential.

The swelling percentages of the CMC solutions as a function of the suspension pH is given in Fig. 4. CMC has a cross-linked structure and allows water molecules to penetrate the macromolecular structure starting from strong acid solutions. The swelling is enhanced because the dissociation of CMC is dependent on the pH and reaches a maximum percentage in the neutral region of $\text{pH} = 6\text{--}8$, which is consistent with the results of Bajpai et al. [28]. Beyond this region, the swelling

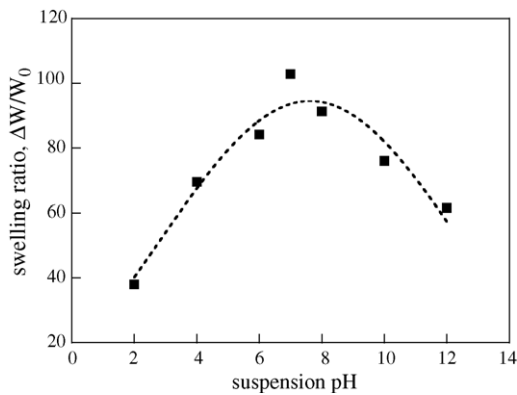


Fig. 4. Swelling ratios of carboxymethyl cellulose solutions as function of hydrogen ion concentration.

percentage decreases with increasing pH. The reduction in swelling in the basic region can be explained by the effect of the increasing number of counter ions in solution. CMC is fabricated by the substitution of a sodium carboxylic group for a hydrogen atom. The sodium ions from the carboxylic group dissolve in water, with the number of ions increasing with pH. The dissociated sodium ions are sufficiently abundant to compress the CMC structure in the basic pH region [28,29].

From the above results, it can be deduced that CMC solutions should be prepared in the neutral pH region of 6–8 to enhance their stability. The increase in swelling ratio relates to an increase in both the cross-linking density and the homogeneity of the network structure [30]. Therefore, a maximum swelling ratio is achieved at pH = 6–8 and the cross linking density and homogeneity of network structure for CMC can be maximum, which enables solid particles to be distributed homogeneously at a higher packing density.

A calculation was made of the time at which the graphite particles suspended in an aqueous medium settle to a depth of 1 cm due to gravity. In order to determine the sedimentation time, the viscosity values were measured using a constant shear rate of 11.9 s^{-1} and are listed in Table 1. The incorporation of both additives into the graphite suspensions retards the sedimentation rate of the graphite particles. This implies that stable graphite suspensions are obtained, even in the aqueous medium. In order to produce uniform dense ceramic green bodies, a stable suspension should be prepared [31–33]. This stability arises by virtue of the combined effect of the CMC and SBR. When comparing the sedimentation times of sus-

Table 1
Calculation of sedimentation time according to Stokes' equation, when graphite particles have settled to a depth of 1 cm

Sample	Formulation	Time ^a (min)
A	Graphite 35 wt. %	9.8
B	Graphite 35 wt. % + CMC 1.5 wt. %	752.4
C	Graphite 35 wt. % + CMC 1.5 wt. % + SBR 1.5 wt. %	795.7

^a To calculate the sedimentation time, viscosity values are measured using a shear rate of 11.9 s^{-1} .

pensions containing CMC and those with CMC and SBR, the latter suspensions take 40 min longer to settle out. This means that CMC coupled with SBR improves the stability of graphite suspensions, which is in good agreement with the electrokinetic results (cf. Fig. 1 with Fig. 3). Recalling the data shown in Table 1, the native graphite suspensions settle out rapidly, which is indicative of suspension instability.

Green graphite anode sheets were coated on to copper substrates. From the above results, the optimum slurry formulation is 35 wt. % graphite with 1.5 wt. % CMC and 1.5 wt. % SBR suspended in water at a suspension pH of 7.5 ± 0.3 in this investigation. Scanning electron micrographs of the as-dried sheets were examined, and the images are shown in Fig. 5. The microstructures of the green sheets containing CMC (Fig. 5A) and both CMC and SBR (Fig. 5B) are shown for direct comparison. The microstructural observations reveal that the graphite sheets with CMC and SBR (Fig. 5B) showed a more homogeneous and less porous microstructure than graphite sheets with CMC alone (Fig. 5A). This is quantitatively confirmed by mercury porosimetry measurements. As can be seen in Fig. 6, it appears that the graphite sheets have smaller-sized pores with a relatively wide distribution when prepared with CMC and SBR, compared with sheets prepared with CMC alone. The latter sheets have pores with a mean diameter of $1.064 \mu\text{m}$, which is twice as large as that of the CMC and SBR sheets that have a mean pore diameter of

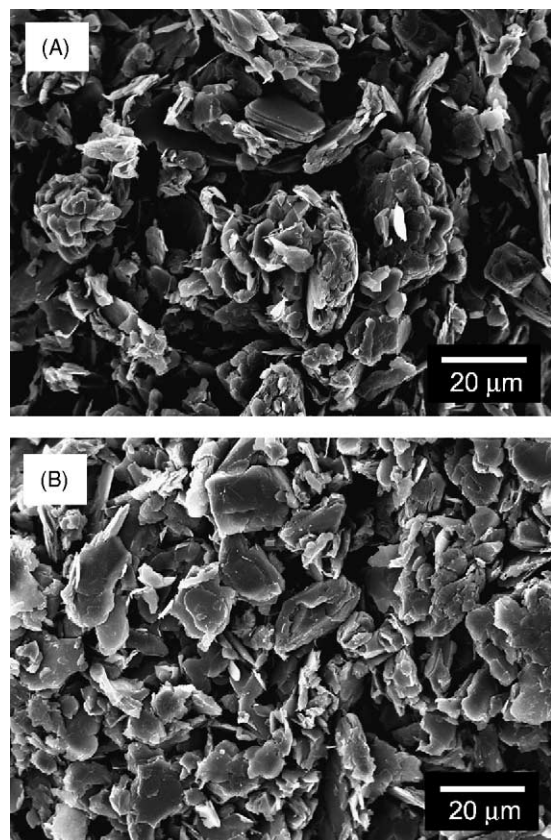


Fig. 5. Scanning electron micrographs of fracture surfaces of graphite anode sheets tape-cast from suspensions with: (A) CMC and (B) CMC plus SBR.

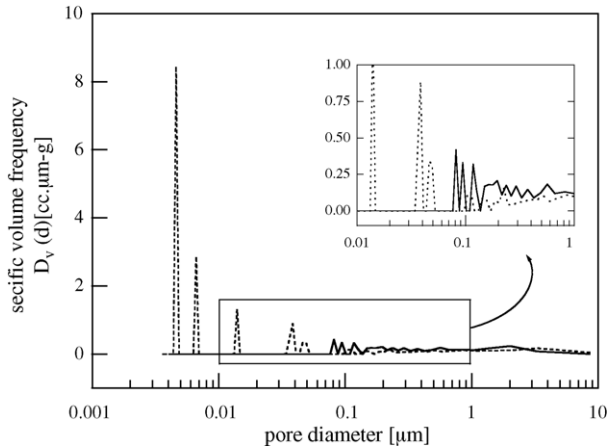


Fig. 6. Pore-size distribution of graphite sheets prepared at fraction of 35 wt.%, where CMC and SBR are added at mass fractions of 1.5% each, based on solids content. The solid and dotted lines indicate samples prepared with CMC and CMC plus SBR, respectively.

0.636 μm . It is concluded that the co-existence of CMC and SBR results in the formation of a denser microstructure with reduced pores by consolidating the particles, and that this leads to a more homogeneous microstructure. As mentioned previously, a homogeneous and dense green microstructure results from an improvement in the stability of graphite particles. These results are confirmed by the earlier experimental findings on the electrokinetic behaviour and the sedimentation time of the graphite suspensions. Thus, highly stable graphite suspensions can be successfully fabricated, even in water-based systems, which may facilitate homogeneous packing. It should be emphasized that the successful aqueous fabrication of a highly-packed, homogeneous graphite sheet can be achieved by an improvement in the dispersion stability of the graphite suspension due to the electrostatic surface potential of the particles that is induced by the repulsive interaction between the CMC and the SBR.

The initial charge–discharge capacity of natural graphite electrodes was measured to evaluate the half-cell characteristics. For comparison, an artificial graphite electrode was prepared using a conventional method that consisted of non-aqueous processing of graphite particulates with a PVDF binder. The initial voltage–capacity curves obtained from the half-cells with natural and artificial graphite electrodes are presented in Fig. 7. During the first charging (intercalation) stage, the potential drops rapidly after a subtle retardation at about $0.8 V_{\text{Li/Li}^+}$. The main intercalation and de-intercalation of lithium occurred at potentials below $0.2 V_{\text{Li/Li}^+}$, accompanied by three potential plateaux. The charge consumed upon the first charging is not fully recovered in the following discharge stage for both the electrodes. The non-recovered capacity is called the ‘irreversible capacity’, which is more or less observed in the first charge–discharge cycle of any carbonaceous material. In the second and subsequent cycles, both graphite electrodes exhibit good reversibility, with a coulombic efficiency of about 100%.

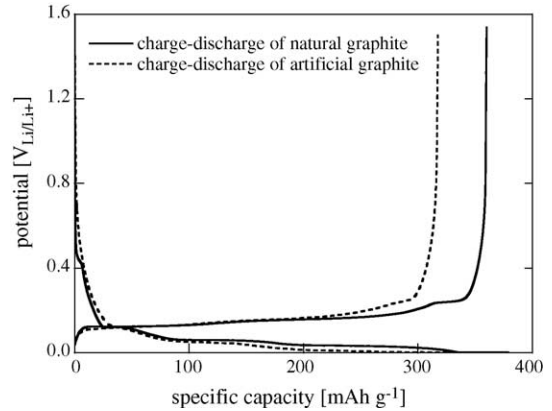


Fig. 7. First charge–discharge curves of natural and artificial graphite anodes prepared using aqueous method and conventional non-aqueous method, respectively, in a 1.1 M LiPF_6 EC/EMC/DMC (30/60/10 vol.%) solution.

According to previous work [34], anodes containing carbonaceous material obtained by powdering giant crystals, such as natural graphite that is highly graphitized, decomposes the non-aqueous electrolyte, with the result that it decreases the capacity and the charge–discharge efficiency of the battery. By contrast, the natural graphite electrode examined here displays a first discharge capacity of $>340 \text{ mAh g}^{-1}$ and a coulombic efficiency $>92\%$ in the first charge–discharge cycle, which is higher than the values for artificial graphite electrodes prepared by the conventional non-aqueous method. The higher reversibility of the natural electrode prepared using an aqueous process can be accounted for in terms of the enhanced effect of the ionic conducting polymer film on the surface of the graphite particles, as this can block the co-intercalation of solvated Li^+ ions. This introduces an elastic component to the solid electrolyte interface (SEI) films formed on the graphite.

The rate behaviour of natural graphite electrodes prepared via an aqueous method is illustrated in Fig. 8. The 750-mAh lithium-ion batteries were charged to the fully charged state (4.2 V) using a constant current (CC)–constant voltage (CV)

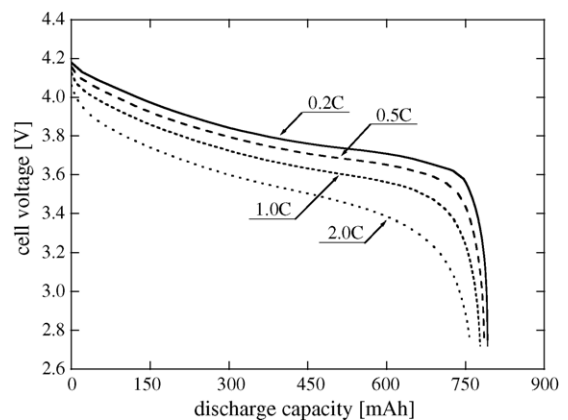


Fig. 8. Discharge curves of 750-mAh lithium-ion cell at various C rates. The cell employs the natural graphite anode prepared by the aqueous process.

protocol. These were then discharged to a voltage of 2.75 V at different rates. For discharge rates of 1.0 and 2.0 C, >90% of the discharge capacity at a low discharge rate of 0.2 C could be recovered. From our electrochemical experiments, natural graphite-based cells fabricated by an aqueous process are very attractive for innovative rechargeable lithium battery systems. The safety and cycle-life times at the cell level, the most critical design criteria for all consumer batteries, are being investigated and the results will be published at a future date.

4. Conclusions

The effect of organic additives on the aqueous processing of natural graphite particulates for lithium-ion battery anodes has been investigated. The stability of the graphite particles is found to be dependent on the electrostatic surface potential of the particles, which is developed by an increase in the near-surface fraction of carboxylate sites. It is caused by repulsive-induced partial rotation of the carboxymethyl side-groups in CMC due to the mutual repulsion between CMC and SBR. An aqueous natural graphite anode for a lithium-ion battery can be successfully fabricated with a homogeneous and dense microstructure, which is confirmed by the green microstructural observation and mercury porosimetry measurements. The electrochemical performance of lithium-ion batteries fabricated by the aqueous processing of graphite particulate shows good rate capability and specific energy density. In addition, the initial specific capacity of above 340 mAh g⁻¹ makes these natural graphite electrodes attractive for use as anodes in innovative rechargeable lithium battery systems.

Acknowledgment

This work was financially supported by the Samsung Advanced Institute of Technology and the Korea Institute Science and Technology Evaluation and Planning (KISTEP) through the National Research Laboratory (NRL) program.

References

- [1] M. Yoo, C.W. Frank, S. Mori, *Chem. Mater.* 15 (2003) 850–861.
- [2] U. Paik, S. Lee, V.A. Hackley, *J. Am. Ceram. Soc.* 86 (2003) 1662–1668.
- [3] H. Shi, *J. Power Sources* 75 (1998) 64–72.
- [4] D. Aurbach, H. Teller, M. Koltypin, E. Levi, *J. Power Sources* 119–121 (2003) 2–7.
- [5] C. Menachem, Y. Wang, J. Flowers, E. Peled, S.G. Greenbaum, *J. Power Sources* 76 (1998) 180–185.
- [6] J. Drofenik, M. Gaberscek, R. Dominko, F.W. Poulsen, M. Mogenssen, S. Pejovnik, J. Jamnik, *Electrochim. Acta* 48 (2003) 883–889.
- [7] X. Zhang, P.N. Ross Jr., R. Kosteci, F. Kong, S. Sloop, J.B. Kerr, K. Striebel, E.J. Cairns, F. McLarnon, *J. Electrochem. Soc.* 148 (2001) 463–470.
- [8] C. Clasen, W.-M. Kulicke, *Prog. Polym. Sci.* 26 (2001) 1839–1919.
- [9] S. Horner, J. Puls, B. Saake, E.-A. Klotz, H. Thielking, *Carbohydr. Polym.* 40 (1999) 1–7.
- [10] C.W. Hoogendam, A. de Keizer, M.A. Cohen Stuart, B.H. Bijsterbosch, J.G. Batelaan, P.M. van der Horst, *Langmuir* 14 (1998) 3825–3839.
- [11] T. Heinze, *Macromol. Chem. Phys.* 199 (1998) 2341–2364.
- [12] O.E. Wolff, US Patent Grant No. 4047289 (1977).
- [13] J. Drofenik, M. Gaberscek, R. Dominko, M. Bele, S. Pejovnik, *J. Power Sources* 94 (2001) 97–101.
- [14] Y.M. Choi, U. Paik, K.H. Kim, US Patent RC-200306-002-1-USO (2003).
- [15] N. Reiji, Y. Kiyoto, S. Masami, S. Masaki, Japanese Patent Grant No. 2003-282147 (2003).
- [16] I. Yoji, N. Hiroyoshi, M. Yuji, Japanese Patent Grant No. 1993-225982 (1993).
- [17] R.G. Horn, *J. Am. Ceram. Soc.* 73 (1990) 1117–1135.
- [18] H.C. Park, J.W. Kim, U. Paik, S.C. Choi, *J. Kor. Ceram. Soc.* 36 (1999) 97–105.
- [19] H.L. Lewis, T. Danko, A. Himy, W. Johnson, *J. Power Sources* 80 (1999) 61–65.
- [20] H. Dietz, J. Garche, K. Wiesener, *J. Power Sources* 14 (1985) 305–319.
- [21] R.A. Wach, H. Mitomo, N. Nagasawa, F. Yoshii, *Radiation Phys. Chem.* 68 (2003) 771–779.
- [22] U. Paik, V.A. Hackley, H.W. Lee, *J. Am. Ceram. Soc.* 82 (1999) 833–840.
- [23] V.A. Hackley, U. Paik, in: V.A. Hackley, J. Texter (Eds.), *Ultrasonic and Dielectric Characterization Techniques for Suspended Particulates*, American Ceramic Society, Westerville, OH, 1998, pp. 191–204.
- [24] S. Wang, in: J.E. Mark (Ed.), *Polymer Data Handbook*, University of Cincinnati, USA, 1998, pp. 983–986.
- [25] J.A. Lewis, *J. Am. Ceram. Soc.* 83 (2000) 2341–2359.
- [26] U. Kästner, H. Hoffmann, R. Dönges, J. Hilbig, *Coll. Surf. A: Physicochem. Eng. Asp.* 123/124 (1997) 307–328.
- [27] J.H. Holtz, J.S.W. Holtz, C.H. Munro, S.A. Asher, *Anal. Chem.* 70 (1998) 780–791.
- [28] A.K. Bajpai, A. Giri, *Carbohydr. Polym.* 53 (2003) 271–279.
- [29] P. Liu, M. Zhai, J. Li, J. Peng, J. Wu, *Radiation Phys. Chem.* 63 (2002) 525–528.
- [30] T. Mitsumata, Y. Suemitsu, K. Fujii, T. Fujii, T. Taniguchi, K. Koyama, *Polymer* 44 (2003) 7103–7111.
- [31] B.V. Velamakanni, J.C. Chang, F.F. Lange, D.S. Pearson, *Langmuir* 6 (1990) 1323–1325.
- [32] M. Okuyama, G.J. Garvey, T.A. Ring, J.S. Haggerty, *J. Am. Ceram. Soc.* 72 (1989) 1918–1924.
- [33] M.D. Sacks, T.Y. Tseng, *J. Am. Ceram. Soc.* 67 (1984) 526–532.
- [34] D. Aurbach, in: W.A. van Schalkwijk, B. Scrosati (Eds.), *Advances in Lithium-Ion Batteries*, Kluwer Academic/Plenum Publishers, NY, 2002, pp. 7–77.